Current Optics and Photonics
Vol. 1, No. 4, August 2017, pp. 372-377

ISSN: 2508-7266(Print) / ISSN: 2508-7274(Online)
DOI: https://doi.org/10.3807/COPP.2017.1.4.372

Effects of Organic Thin Films on Local Resonance of Metamaterials under Photoexcitation

Myeong-Seong Song[1], In-Wook Hwang[2], Chang-Lyoul Lee[2], Chul Kang[2], Chul-Sik Kee[2], Sae June Park[3], Yeong Hwan Ahn[3], Doo Jae Park[4], and Joong Wook Lee[1]*

[1]Department of Physics and Optoelectronics Convergence Research Center, Chonnam National University, Gwangju 61186, Korea
[2]Advanced Photonics Research Institute, GIST, Gwangju 61005, Korea
[3]Department of Physics and Department of Energy Systems Research, Ajou University, Suwon 16499, Korea
[4]Department of Physics, Hallym University, Chuncheon 24252, Korea

(Received March 2, 2017 : revised June 2, 2017 : accepted June 2, 2017)

We demonstrate that the local resonance of metamaterials can be tuned by the effects of organic thin films under photoexcitation. Tris (8-hydroxyquinolinato) aluminum (Alq_3) layers are deposited on metamaterial/silicon hybrid structures. By varying the thickness of the Alq_3 layer on the subwavelength scale, the resonant peak of the metamaterial becomes very adjustable, due to the effect of a thin dielectric substrate. In addition, under photoexcitation all the spectral peaks of the resonance shift to higher frequencies. This originates from the reduction of the capacitive response generated inside the gaps of split-ring resonators. The adjustability of the electromagnetic spectrum may be useful for developing optical systems requiring refractive-index engineering and active optical devices.

Keywords : Organic materials, Modulators, Terahertz spectroscopy, Metamaterials, Optical devices
OCIS codes : (160.4890) Organic materials; (300.6495) Spectroscopy, terahertz; (230.4110) Modulators; (160.3918) Metamaterials; (230.0230) Optical devices

I. INTRODUCTION

Terahertz-related technologies have received a lot of attention, due to their possible use in various fields such as high-speed communication, spectroscopic/imaging systems, and medical applications [1-5]. Among those, extensive research has been conducted to develop optical devices, such as filters and modulators, working at terahertz (THz) frequencies [6-8]. Actively controlling THz waves with improved functionality is necessary to realize the potential of optical devices. Much research has been carried out to investigate optical control of the spatial location, polarization, phase, propagation direction, and amplitude of reflected and transmitted THz waves, using a variety of materials and structures [9-18]. In particular, active THz modulation based on organic/inorganic hybrid structures has been suggested for realizing high modulation efficiency, caused by the change in optical properties due to the dynamics of photoexcited carriers at the interfaces of the hybrid structures [16, 17].

Recently, experimentally tuning the resonant response of artificially structured materials (known as metamaterials) has become a topic of interest, due to the possibilities of developing active THz devices for specific requirements [19-21]. In particular, using dielectric thin films with subwavelength thicknesses, a remarkable modification of the resonance was theoretically proposed and experimentally observed [22, 23]. The underlying mechanism of the phenomenon is the degree of a dielectric thin layer's contribution when interacting with metamaterial structures. To take advantage of this technique in practice, the characteristics of the resonance shifts of metamaterials should be investigated for a variety of materials and structures, and

*Corresponding author: leejujc@chonnam.ac.kr

Color versions of one or more of the figures in this paper are available online.

an effective method for actively controlling the resonance should be suggested.

In this paper we experimentally observe the resonance shifts of metamaterials in organic/metamaterial/silicon hybrid structures, by varying the subwavelength thickness of organic thin film, and by exciting carriers on a silicon substrate under photoexcitation. The transmission properties of organic/metamaterial/silicon structures with different layer thickness of tris (8-hydroxyquinolinato) aluminum (Alq_3) are measured using THz time-domain spectroscopy under externally excited laser irradiation. The dramatic shift of the resonance frequency due to the change in thickness of the Alq_3 layer indicates that the contribution of organic thin layers when interacting with the metamaterial/silicon structures is highly sensitive to the subwavelength thickness. In addition, the blueshift of the resonant frequency under photoexcitation shows that the fundamental inductive-capacitive resonance can be tuned by changing the effective capacitance generated inside the gaps of combined split-ring resonators (SRRs). Our simulation results also argue that the degree of resonant-frequency shift due to photoexcitation depends on each resonance mode.

II. METHODS

Figure 1(a) shows the schematic of an experimental THz wave transmission through organic/metamaterial/silicon hybrid structures under laser light irradiation. The side view of a typical element shows the metamaterial inclusion structure, sandwiched by organic and silicon (Si) substrates, as schematically depicted in Fig. 1(b). All samples are fabricated on a 500 μm thick inorganic layer of highly resistive Si (1.0×10^5 Ω cm). The metamaterial structures are deposited on the Si substrate using a conventional photolithographic technique, forming metal patterns of Cr and Au (2 nm/150 nm approx.). Figure 1(c) shows the geometry and dimensions of a THz metamaterial's unit cell. The unit element consists of two single SRRs, back to back. The two gaps formed on the sides have a fixed gap size a of 2 μm and a length b of the metallic bar of 7 μm. The width of all wires w is 4 μm. The side lengths m and n of the square unit element are 76 μm. The basic elements are arranged with periods P_x and P_y of 100 μm throughout the whole metamaterial area of 10×10 mm^2. The metamaterial layer is used as a frequency-selective surface, selectively transmitting incident THz waves at specific frequencies. The resonant response is determined by the fundamental LC resonance due to the values of an inductance L and a capacitance C, which are provided by the structural dimensions of the SRRs. Here a net electric response becomes prominent, since the two symmetric inductive loops make the magnetic response negligible.

The third layer shown in Fig. 1(b) is a thin organic layer, consisting of Alq_3 molecules (99.9%) from Organic Semiconductor Materials (OSM) [24, 25]. To fabricate an ultrathin dielectric substrate on the top of the metamaterial/silicon structures, the Alq_3 molecules are deposited using a vacuum thermal evaporation method (10^{-6} torr) at room temperature. Alq_3 layers with different thicknesses (t_1 = 0, 1, 5, and 10 μm) are fabricated by controlling the evaporation rate.

The transmittance of THz waves is measured using a typical THz time-domain spectroscopy system [26-28]. The optically induced THz radiation from a biased photo-conductive antenna transmits through the samples, and is detected by a THz photoconductive antenna. The polarization direction of incident THz waves is set to zero at the configuration shown in Fig. 1(a). We obtain the transmitted time-domain waveforms with (or without) photoexcitation, which is generated using a CW diode laser of wavelength 785 nm and intensity 200 mW. The diameters of the focused THz waves and optical pump beams are consistently ~3 mm.

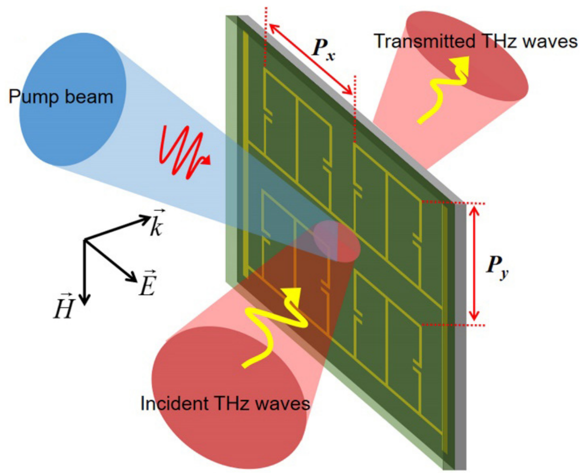

(a)

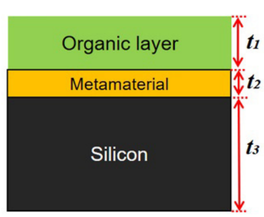

(b)

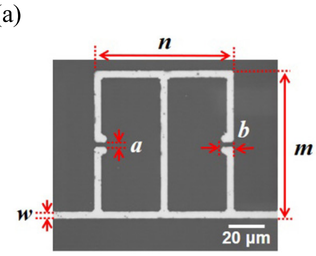

(c)

FIG. 1. (a) Schematic of the organic/metamaterial/silicon hybrid structure, and experimental configuration for THz transmission measurements. The polarization of incident THz waves is set zero for this configuration. The optical pump beam and incident THz waves impinge upon the same area of the sample surface; (b) The side view of a three-layered structure consisting of organic, metamaterial, and Si. The thicknesses of the Si and metamaterial layers are t_3 = 500 μm and t_2 = 100 nm respectively. The thickness of the organic layer is varied from t_1 = 0 μm to t_1 = 10 μm; (c) Optical image of a unit cell of the metamaterial sandwiched by organic and Si layers. The unit cell has dimensions of a = 2 μm, b = 7 μm, m = n = 76 μm, and w = 4 μm.

The THz spectra in the range of 0.1-1.2 THz are obtained by applying a fast Fourier transform method to the measured time-domain waveforms.

III. RESULTS AND DISCUSSION

Figure 2 shows the measured transmission spectra for four samples with different thicknesses, obtained without Fig. 2(a) and with Fig. 2(b) photoexcitation. The polarization of the incident THz waves is parallel to the wires in the middle. Two distinct resonances are clearly observed in both cases. Whether an optical beam impinges on the surface of the samples or not, the resonances show frequency-dependent response as a function of thickness t_1, which once more verifies the previous results showing the change of electric

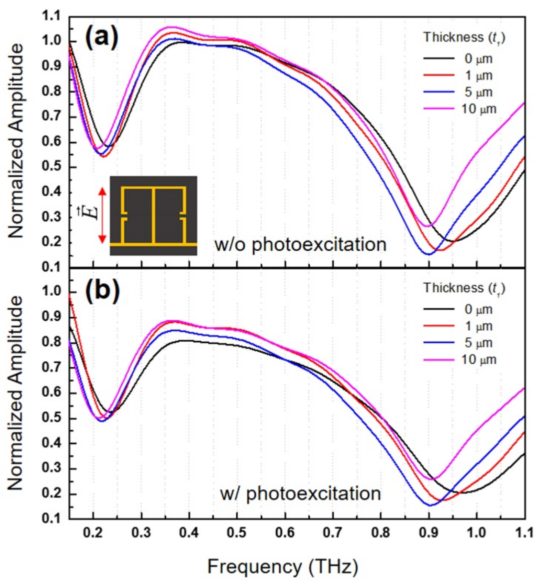

FIG. 2. Terahertz-wave transmission spectra of four samples with different thicknesses of the organic thin film, obtained (a) without and (b) with photoexcitation. The inset shows the direction of polarization of the incident THz waves.

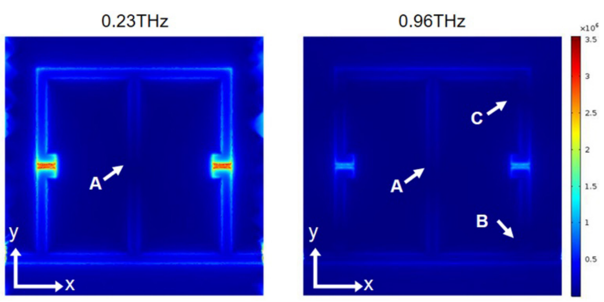

(a) (b)

FIG. 3. Simulated electric-field amplitude distributions at the top surface of the sample obtained at the two spectral peaks, (a) 0.23 THz and (b) 0.96 THz, of the resonances.

response on ultrathin dielectric substrates [20, 23]. When the Alq_3 layer is absent from the metamaterial/silicon hybrid structure, the resonant peaks are located in the relatively highest-frequency region. With increasing thickness of the Alq_3 layer upon the metamaterial/silicon hybrid structure, the resonant peaks shift continuously toward lower frequencies.

First, to understand the origin of the two resonances, simulations of the structures are carried out at the two spectral peaks of 0.23 and 0.96 THz. We numerically investigate the near-electric-field distribution using COMSOL Multiphysics software. The simulations are performed on the metamaterial structures surrounded by perfectly matched layers in the direction perpendicular to the surface, and with periodic boundary conditions in the planes of the films. Figure 3 shows the simulated electric-field distributions obtained at the two resonant peaks on the top surfaces of the samples.

Each metamaterial unit cell is structurally symmetric about the wire in the middle. As a result, the center of the structures (marked by point A) acts as an electric-field node for both cases of the two resonances. On the other hand, the induced capacitance at the SRR gaps enables the flow of displacement current through the edges of the metallic wires, acting as electric-field antinodes. The resonance at 0.23 THz is therefore related to the fundamental inductive-capacitive response induced by circulating currents on the gross metallic area of each unit element. The electric field distribution at 0.96 THz shows three distinct nodal points, marked A, B, and C. The resonance can be regarded as the next-higher resonance mode generated by the change in capacitance at the gaps.

To reliably assure the change in spectral characteristics of the resonances of metamaterials, the values of spectral resonances are extracted and plotted as a function of the thicknesses of the organic thin layers for both cases, with and without photoexcitation, as shown in Fig. 4. The resonance shift to lower frequencies strongly supports the assertion that the effective substrate index of the organic thin layer stands out with increasing thickness of the organic film [22]. Note that all resonant peaks shift to higher frequencies under photoexcitation. The unit cell of the metamaterial composed of SRRs shows two metallic loops and two air gaps. The loops and gaps generate the loop inductance L and the gap capacitance C respectively. In general, the fundamental resonant frequency of the metamaterials is therefore given approximately by the inductive-capacitive resonance (LC resonance), [29-31]. The values of L and C can be varied with the structural dimensions of the total length of the metallic loops and the width of the air gap. This means that the resonant frequency due to the LC response can be controlled by properly designing the structure of the SRRs. In addition, change in the properties of surrounding materials leads to change in values of gap capacitance and loop inductance. The photo-excited carriers (generated at the substrate by the impinging optical beam) reduce the capacitive response

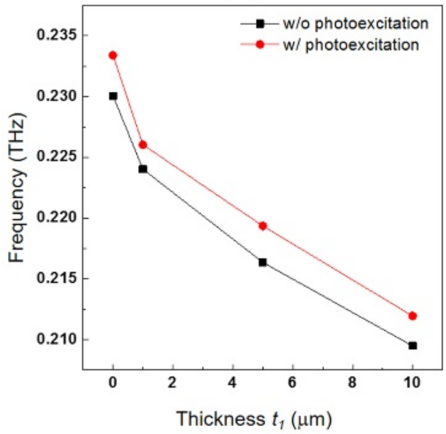

(a)

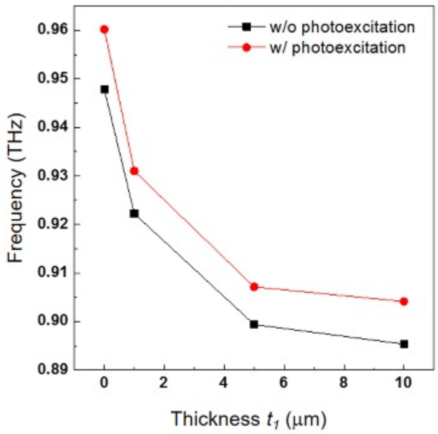

(b)

FIG. 4. Extracted values of the spectral resonances as a function of the thickness of the organic thin layer, at (a) the fundamental and (b) the next-higher resonance modes, for both cases with (red circles) and without (black squares) photoexcitation. The polarization of the incident THz waves is along the *y*-axis.

associated with the SRR gaps. On the basis of the fundamental *LC* resonance, the reduction of the capacitive response leads to the blueshift of the resonance.

Next, we make a brief comparison between the results demonstrated above and the experimental data measured under *x*-axis polarization of incident THz waves, shown in Figs. 5(a) and 5(b). Figure 5(c) shows the extracted values of the spectral resonances observed under the condition of *x*-axis polarization of the THz waves. This clearly shows that, as for the results measured under *y*-axis polarization, the resonance value shifts to higher frequency with decreasing thickness of the organic thin film on the metamaterial structures. In contrast, the blueshift phenomenon of the resonances with photoexcitation is not relatively clear, compared to the results shown in Fig. 4. This implies that the change of the capacitive response inside the SRR gaps scarcely contributes to change in spectral characteristics of the local resonance due to the metamaterial structure. This

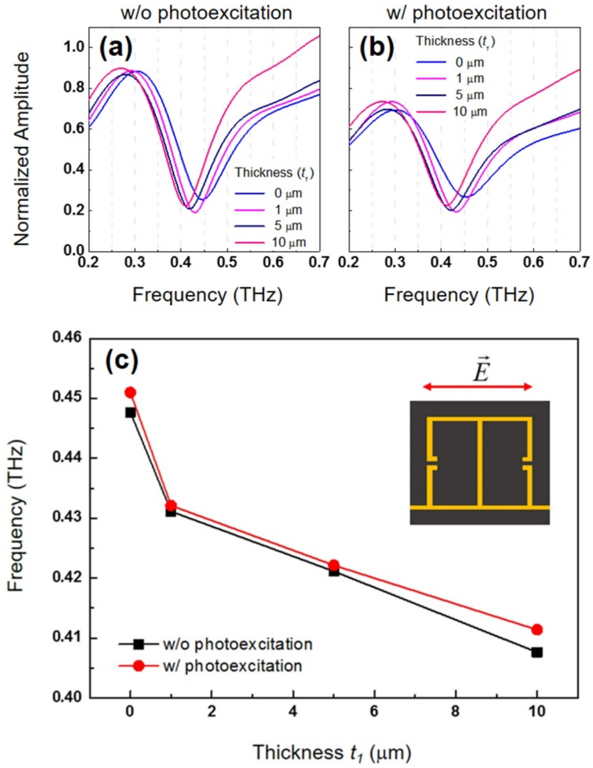

FIG. 5. Terahertz-wave transmission spectra of four samples with different thicknesses of the organic thin film, obtained (a) without and (b) with photoexcitation, measured under *x*-axis polarization. (c) Extracted values of the spectral resonances as a function of the thickness of the organic thin layer for both cases with (red circles) and without (black squares) photoexcitation. The polarization of the incident THz waves is along the *x*-axis, which is perpendicular to the polarization direction used to obtain the results shown in Fig. 4.

is due to the fact that the resonance appearing at 0.43 THz originates from the electric-dipole resonance occurring in the straight metal wires lying along the *x*-axis. In this situation, the SRR gaps would have difficulty functioning as local capacitors.

IV. CONCLUSION

In conclusion, we demonstrate that the local resonances in organic/metamaterial/Si hybrid structures can be tuned not only by varying the thickness of the organic thin film, but also by controlling the photoexcitation condition. The redshift of the resonances occurring when the thickness of the organic thin layer increases (on the subwavelength scale) is associated with the effect of a thin dielectric substrate. The blueshift of the resonances under photoexcitation is due to the reduction of capacitive response by the photo-excited carriers generated at the substrate. This is explained on the basis of the fundamental inductive-capacitive resonance. These results offer invaluable insights into exploiting metamaterial-based hybrid structures for developing optical systems requiring refractive-index engineering and active optical devices.

ACKNOWLEDGMENT

This research was supported by the Basic Science Research Program through the National Research Foundation of Korea (NRF), which is funded by the Ministry of Education, Science and Technology and the Korea government (MSIP) (NRF-2014R1A1A2057920; NRF-2016R1D1A1B03935241; NRF-2016R1A2B4013003). This study was also financially supported by the GIST Research Institute (GRI) and Chonnam National University in 2017.

REFERENCES

1. Y. S. Lee, "Principles of terahertz science and technology," Springer, New York (2009).
2. M. Tonouchi, "Cutting-edge terahertz technology," Nat. Photonics **1**, 97-105 (2007).
3. D. M. Mittleman, M. Gupta, R. Neelamani, R. G. Baraniuk, J. V. Rudd, and M. Koch, "Recent advances in terahertz imaging," Appl. Phys. B **68**, 1085-1094 (1999).
4. P. H. Siegel, "Terahertz technology," IEEE Trans. Microw. Theory. Tech. **50,** 910-928 (2002).
5. B. Ferguson and X.-C. Zhang, "Materials for terahertz science and technology," Nat. Mater. **1,** 26-33 (2002).
6. H. Cao and A. Nahata, "Coupling of terahertz pulses onto a single metal wire waveguide using milled grooves," Opt. Express **13**, 7028-7034 (2005).
7. J. W. Lee, M. A. Seo, D. J. Park, D. S. Kim, S. C. Jeoung, C. Lienau, Q. H. Park, and P. C. M. Planken, "Shape resonance omni-directional terahertz filters with near-unity transmittance," Opt. Express **14**, 1253 (2006).
8. W. J. Padilla, A. J. Taylor, C. Highstrete, M. Lee, and R. D. Averitt, "Dynamical electric and magnetic metamaterial response at terahertz frequencies," Phys. Rev. Lett. **96**, 107401 (2006).
9. J. N. Heyman, R. Kersting, and K. Unterrainer, "Time-domain measurement of intersubband oscillations in a quantum well," Appl. Phys. Lett. **72**, 644-646 (1998).
10. I. H. Libon, S. Baumgärtner, M. Hempel, N. E. Hecker, J. Feldmann, M. Koch, and P. Dawson, "An optically controllable terahertz filter," Appl. Phys. Lett. **76**, 2821-2823 (2000).
11. T. Kleine-Ostmann, P. Dawson, K. Pierz, G. Hein, and M. Koch, "Room-temperature operation of an electrically driven terahertz modulator," Appl. Phys. Lett. **84**, 3555-3557 (2004).
12. H.-T.Chen, W. J. Padilla, J. M. O. Zide, A. C. Gossard, A. J. Taylor, and R. D. Averitt, "Active terahertz metamaterial devices," Nature **444**, 597-600 (2006).
13. E. Hendry, M. J. Lockyear, J. Gómez Rivas, L. Kuipers, and M. Bonn, "Ultrafast optical switching of the THz transmission through metallic subwavelength hole arrays," Phys. Rev. B **75**, 235305 (2007).
14. E. Hendry, F. J. Garcia-Vidal, L. Martin-Moreno, J. Gómez Rivas, M. Bonn, A. P. Hibbins, and M. J. Lockyear, "Optical control over surface-plasmon-polariton-assisted THz transmission through a slit aperture," Phys. Rev. Lett. **100**, 123901 (2008).
15. H.-T. Chen, W. J. Padilla, M. J. Cich, A. K. Azad, R. D. Averitt, and A. J. Taylor "A metamaterial solid-state terahertz phase modulator," Nat. Photonics **3**, 148-151 (2009).
16. H. K. Yoo, C. Kang, Y. W. Yoon, H. J. Lee, J. W. Lee, K. Lee, and C. S. Kee, "Organic conjugated material-based broadband terahertz wave modulators," Appl. Phys. Lett. **99**, 061108 (2011).
17. H. K. Yoo, Y. W. Yoon, K. Lee, C. Kang, C. S. Kee, I. W. Hwang, and J. W. Lee, "Highly efficient terahertz wave modulators by photo-excitation of organics/silicon bilayers," Appl. Phys. Lett. **105**, 011115 (2014).
18. D. G. Cooke and P. U. Jepsen, "Optical modulation of terahertz pulses in a parallel plate waveguide," Opt. Express **16**, 15123-15129 (2008).
19. M. Liu, H. Y. Hwang, H. Tao, A. C. Strikwerda, K. Fan, G. R. Keiser, A. J. Sternbach, K. G. West, S. Kittiwatanakul, J. Lu, S. A. Wolf, F. G. Omenetto, X. Zhang, K. A. Nelson, and R. D. Averitt, "Terahertz-field-induced insulator-to-metal transition in vanadium dioxide metamaterial," Nature **487**, 345-348 (2012).
20. H. Tao, A. C. Strikwerda, M. Liu, J. P. Mondia, E. Ekmekci, K. Fan, D. L. Kaplan, W. J. Padilla, Z. Zhang, R. D. Averitt, and F. G. Omenetto, "Performance enhancement of terahertz metamaterials on ultrathin substrates for sensing applications," Appl. Phys. Lett. **97**, 261909 (2010).
21. Z. C. Chen, M. H. Hong, C. S. Lim, N. R. Han, L. P. Shi, and T. C. Chong, "Parallel laser microfabrication of large-area asymmetric split ring resonator metamaterials and its structural tuning for terahertz resonance," Appl. Phys. Lett. **96**, 181101 (2010).
22. D. J. Park, M. S. Jeong, and S. B. Choi, "Effect of a dielectric substrate with a subwavelength thickness of light diffraction by rectangular hole arrays on metallic film," J. Kor. Phys. Soc. **65**, 1390-1398 (2014).
23. S. J. Park, S. A. N. Yoon, and Y. H. Ahn, "Dielectric constant measurements of thin films and liquids using terahertz metamaterials," RSC. Adv. **6**, 69381-69386 (2016).
24. A. Lukyanov and D. Andrienko, "Extracting nondispersive charge carrier mobilities of organic semiconductors from simulation of small systems," Phys. Rev. B **82**, 193202 (2010).
25. M. M. El-Nahass, A. M. Farid, and A. A. Atta, "Structural and optical properties of Tris (8-hydroxyquinoline) aluminum (III) (Alq_3) thermal evaporated thin films," J. All. Com. **507**, 112-119 (2010).
26. M. van Exter and D. Grischkowsky, "Optical and electric properties of doped silicon from 0.1 to 2 THz," Appl. Phys. Lett. **56**, 1694-1696 (1990).
27. Z. Jiang, M. Li, and X. C. Zhang, "Dielectric constant measurement of thin films by differential time domain spectroscopy," Appl. Phys. Lett. **76**, 3221-3223 (2000).
28. J. W. Lee, J. K. Yang, I. B. Sohn, H. K. Choi, C. Kang, and C. S. Kee, "Relationship between the order of rotation symmetry in perforated apertures and terahertz transmission characteristics," Opt. Eng. **51**(11), 119002 (2012).
29. C. G. Hu, M. B. Pu, X. Li, M. Wang, Q. Feng, and X. G.

Luo, “Extraordinary optical transmission induced by electric resonance ring and its dynamic manipulation at far-infrared regime,” Opt. Express **19**, 18109-18115 (2011).
30. R. Singh, A. K. Azad, Q. X. Jia, A. J. Taylor, and H. T. Chen, “Thermal tunability in terahertz metamaterials fabricated on strontium titanate single-crystal substrates,” Opt. Lett. **36**, 1230-1232 (2011).
31. Y. Yang, R. Huang, L. Cong, Z. Zhu, J. Gu, Z. Tian, R. Singh, S. Zhang, J. Han, and W. Zhang, “Modulating the fundamental inductive-capacitive resonance in asymmetric double-split ring terahertz metamaterials,” Appl. Phys. Lett. **98**, 121114 (2011).